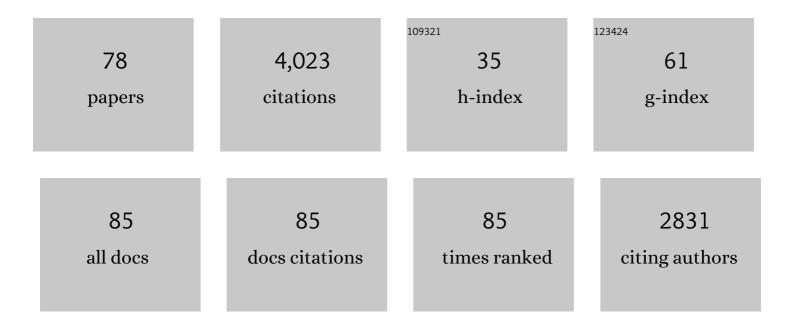
List of Publications by Year in descending order

Source: https://exaly.com/author-pdf/7776895/publications.pdf Version: 2024-02-01



SONCCHAO CHEN

#	Article	IF	CITATIONS
1	Hand-feel soil texture observations to evaluate the accuracy of digital soil maps for local prediction of soil particle size distribution: A case study in Central France. Pedosphere, 2023, 33, 731-743.	4.0	5
2	Digital soil mapping of organic carbon at two depths in loess hilly region of Northern Iran. , 2022, , 467-475.		2
3	Digital mapping of GlobalSoilMap soil properties at a broad scale: A review. Geoderma, 2022, 409, 115567.	5.1	167
4	Soil organic carbon storage, distribution, and influencing factors at different depths in the dryland farming regions of Northeast and North China. Catena, 2022, 210, 105934.	5.0	18
5	Fusion of visible-to-near-infrared and mid-infrared spectroscopy to estimate soil organic carbon. Soil and Tillage Research, 2022, 217, 105284.	5.6	21
6	Drivers of water erosion-induced lateral soil carbon loss on the Tibetan Plateau. Catena, 2022, 211, 105970.	5.0	7
7	Comparison of near-infrared, mid-infrared, Raman spectroscopy and near-infrared hyperspectral imaging to determine chemical, structural and rheological properties of apple purees. Journal of Food Engineering, 2022, 323, 111002.	5.2	9
8	Role of Environment Variables in Spatial Distribution of Soil C, N, P Ecological Stoichiometry in the Typical Black Soil Region of Northeast China. Sustainability, 2022, 14, 2636.	3.2	5
9	Strategies for efficient estimation of soil organic content at the local scale based on a national spectral database. Land Degradation and Development, 2022, 33, 1649-1661.	3.9	6
10	Comparing Two Different Development Methods of External Parameter Orthogonalization for Estimating Organic Carbon from Field-Moist Intact Soils by Reflectance Spectroscopy. Remote Sensing, 2022, 14, 1303.	4.0	6
11	Hand-feel soil texture and particle-size distribution in central France. Relationships and implications. Catena, 2022, 213, 106155.	5.0	12
12	Fruit variability impacts puree quality: Assessment on individually processed apples using the visible and near infrared spectroscopy. Food Chemistry, 2022, 390, 133088.	8.2	7
13	Improving remote sensing of salinity on topsoil with crop residues using novel indices of optical and microwave bands. Geoderma, 2022, 422, 115935.	5.1	6
14	Digital Mapping of Soil Organic Carbon with Machine Learning in Dryland of Northeast and North Plain China. Remote Sensing, 2022, 14, 2504.	4.0	9
15	Preliminary risk assessment of regional industrial enterprise sites based on big data. Science of the Total Environment, 2022, 838, 156609.	8.0	9
16	Effectiveness of different approaches for in situ measurements of organic carbon using visible and near infrared spectrometry in the Poyang Lake basin area. Land Degradation and Development, 2021, 32, 1301-1311.	3.9	8
17	A review of the world's soil museums and exhibitions. Advances in Agronomy, 2021, 166, 277-304.	5.2	6
18	Digital mapping of the soil thickness of loess deposits over a calcareous bedrock in central France. Catena, 2021, 198, 105062.	5.0	24

#	Article	IF	CITATIONS
19	Revealing the scale- and location-specific controlling factors of soil organic carbon in Tibet. Geoderma, 2021, 382, 114713.	5.1	39
20	Visible, near- and mid-infrared spectroscopy coupled with an innovative chemometric strategy to control apple puree quality. Food Control, 2021, 120, 107546.	5.5	17
21	Can N ₂ O emissions offset the benefits from soil organic carbon storage?. Global Change Biology, 2021, 27, 237-256.	9.5	174
22	A method using near infrared hyperspectral imaging to highlight the internal quality of apple fruit slices. Postharvest Biology and Technology, 2021, 175, 111497.	6.0	24
23	Soil erosion modelling: A bibliometric analysis. Environmental Research, 2021, 197, 111087.	7.5	78
24	Climate change-induced greening on the Tibetan Plateau modulated by mountainous characteristics. Environmental Research Letters, 2021, 16, 064064.	5.2	16
25	Organic carbon storage potential of cropland topsoils in East China: Indispensable roles of cropping systems and soil managements. Soil and Tillage Research, 2021, 211, 105052.	5.6	8
26	An integrated assessment methodology for management of potentially contaminated sites based on public data. Science of the Total Environment, 2021, 783, 146913.	8.0	21
27	Soil erosion modelling: A global review and statistical analysis. Science of the Total Environment, 2021, 780, 146494.	8.0	261
28	Mid-infrared technique to forecast cooked puree properties from raw apples: A potential strategy towards sustainability and precision processing. Food Chemistry, 2021, 355, 129636.	8.2	4
29	Evaluating validation strategies on the performance of soil property prediction from regional to continental spectral data. Geoderma, 2021, 400, 115159.	5.1	32
30	Diagnosis of cadmium contamination in urban and suburban soils using visible-to-near-infrared spectroscopy. Environmental Pollution, 2021, 291, 118128.	7.5	26
31	Evaluation of Optimized Preprocessing and Modeling Algorithms for Prediction of Soil Properties Using VIS-NIR Spectroscopy. Sensors, 2021, 21, 6745.	3.8	14
32	Monitoring soil organic carbon in alpine soils using in situ visâ€NIR spectroscopy and a multilayer perceptron. Land Degradation and Development, 2020, 31, 1026-1038.	3.9	37
33	Composite assessment of human health risk from potentially toxic elements through multiple exposure routes: A case study in farmland in an important industrial city in East China. Journal of Geochemical Exploration, 2020, 210, 106443.	3.2	37
34	Impacts of national scale digital soil mapping programs in France. Geoderma Regional, 2020, 23, e00337.	2.1	10
35	Improved Mapping of Potentially Toxic Elements in Soil via Integration of Multiple Data Sources and Various Geostatistical Methods. Remote Sensing, 2020, 12, 3775.	4.0	16
36	Current Estimates of Soil Organic Carbon Stocks Are Not Four to Six Times Underestimated. Comment on "Non-Flat Earth Recalibrated for Terrain and Topsoil. Soil Syst. 2018, 2, 64― Soil Systems, 2020, 4, 45.	2.6	0

#	Article	IF	CITATIONS
37	Data fusion for the measurement of potentially toxic elements in soil using portable spectrometers. Environmental Pollution, 2020, 263, 114649.	7.5	36
38	Rapid Determination of Soil Class Based on Visible-Near Infrared, Mid-Infrared Spectroscopy and Data Fusion. Remote Sensing, 2020, 12, 1512.	4.0	25
39	Current status, spatial features, health risks, and potential driving factors of soil heavy metal pollution in China at province level. Environmental Pollution, 2020, 266, 114961.	7.5	257
40	Modelling bioaccumulation of heavy metals in soil-crop ecosystems and identifying its controlling factors using machine learning. Environmental Pollution, 2020, 262, 114308.	7.5	126
41	Fine-Resolution Mapping of Soil Total Nitrogen across China Based on Weighted Model Averaging. Remote Sensing, 2020, 12, 85.	4.0	31
42	Comparing laboratory and airborne hyperspectral data for the estimation and mapping of topsoil organic carbon: Feature selection coupled with random forest. Soil and Tillage Research, 2020, 199, 104589.	5.6	66
43	Model averaging for mapping topsoil organic carbon in France. Geoderma, 2020, 366, 114237.	5.1	52
44	Exploring the potential of airborne hyperspectral image for estimating topsoil organic carbon: Effects of fractional-order derivative and optimal band combination algorithm. Geoderma, 2020, 365, 114228.	5.1	58
45	A comprehensive framework for assessing the impact of potential agricultural pollution on grain security and human health in economically developed areas. Environmental Pollution, 2020, 263, 114653.	7.5	35
46	Rapid determination of soil classes in soil profiles using vis–NIR spectroscopy and multiple objectives mixed support vector classification. European Journal of Soil Science, 2019, 70, 42-53.	3.9	21
47	Multiâ€sensor fusion for the determination of several soil properties in the Yangtze River Delta, China. European Journal of Soil Science, 2019, 70, 162-173.	3.9	79
48	National digital soil map of organic matter in topsoil and its associated uncertainty in 1980's China. Geoderma, 2019, 335, 47-56.	5.1	80
49	Baseline map of soil organic carbon in Tibet and its uncertainty in the 1980s. Geoderma, 2019, 334, 124-133.	5.1	35
50	Cadmium concentration estimation in peri-urban agricultural soils: Using reflectance spectroscopy, soil auxiliary information, or a combination of both?. Geoderma, 2019, 354, 113875.	5.1	45
51	Satellite data integration for soil clay content modelling at a national scale. International Journal of Applied Earth Observation and Geoinformation, 2019, 82, 101905.	2.8	57
52	Improvement of Spatial Modeling of Cr, Pb, Cd, As and Ni in Soil Based on Portable X-ray Fluorescence (PXRF) and Geostatistics: A Case Study in East China. International Journal of Environmental Research and Public Health, 2019, 16, 2694.	2.6	30
53	Simultaneous measurement of multiple soil properties through proximal sensor data fusion: A case study. Geoderma, 2019, 341, 111-128.	5.1	73
54	Evaluation of Machine Learning Approaches to Predict Soil Organic Matter and pH Using vis-NIR Spectra. Sensors, 2019, 19, 263.	3.8	91

#	Article	IF	CITATIONS
55	X-ray fluorescence and visible near infrared sensor fusion for predicting soil chromium content. Geoderma, 2019, 352, 61-69.	5.1	57
56	High-resolution three-dimensional mapping of soil organic carbon in China: Effects of SoilGrids products on national modeling. Science of the Total Environment, 2019, 685, 480-489.	8.0	66
57	Estimating forest soil organic carbon content using vis-NIR spectroscopy: Implications for large-scale soil carbon spectroscopic assessment. Geoderma, 2019, 348, 37-44.	5.1	70
58	Probability mapping of soil thickness by random survival forest at a national scale. Geoderma, 2019, 344, 184-194.	5.1	36
59	National estimation of soil organic carbon storage potential for arable soils: A data-driven approach coupled with carbon-landscape zones. Science of the Total Environment, 2019, 666, 355-367.	8.0	61
60	Identifying heavy metal pollution hot spots in soil-rice systems: A case study in South of Yangtze River Delta, China. Science of the Total Environment, 2019, 658, 614-625.	8.0	90
61	Combination of fractional order derivative and memory-based learning algorithm to improve the estimation accuracy of soil organic matter by visible and near-infrared spectroscopy. Catena, 2019, 174, 104-116.	5.0	81
62	A high-resolution map of soil pH in China made by hybrid modelling of sparse soil data and environmental covariates and its implications for pollution. Science of the Total Environment, 2019, 655, 273-283.	8.0	124
63	Soil carbon stocks under different land uses and the applicability of the soil carbon saturation concept. Soil and Tillage Research, 2019, 188, 53-58.	5.6	71
64	Fine resolution map of top- and subsoil carbon sequestration potential in France. Science of the Total Environment, 2018, 630, 389-400.	8.0	109
65	Current and future assessments of soil erosion by water on the Tibetan Plateau based on RUSLE and CMIP5 climate models. Science of the Total Environment, 2018, 635, 673-686.	8.0	184
66	Building a pedotransfer function for soil bulk density on regional dataset and testing its validity over a larger area. Geoderma, 2018, 312, 52-63.	5.1	48
67	Assessment of important soil properties related to Chinese Soil Taxonomy based on vis–NIR reflectance spectroscopy. Computers and Electronics in Agriculture, 2018, 144, 1-8.	7.7	58
68	Rapid identification of soil organic matter level via visible and near-infrared spectroscopy: Effects of two-dimensional correlation coefficient and extreme learning machine. Science of the Total Environment, 2018, 644, 1232-1243.	8.0	85
69	Heavy Metal Pollution Delineation Based on Uncertainty in a Coastal Industrial City in the Yangtze River Delta, China. International Journal of Environmental Research and Public Health, 2018, 15, 710.	2.6	42
70	THE GLOBALSOILMAP PROJECT: PAST, PRESENT, FUTURE, AND NATIONAL EXAMPLES FROM FRANCE. Dokuchaev Soil Bulletin, 2018, , 3-23.	0.6	5
71	Organic carbon prediction in soil cores using VNIR and MIR techniques in an alpine landscape. Scientific Reports, 2017, 7, 2144.	3.3	37
72	Application of portable XRF and VNIR sensors for rapid assessment of soil heavy metal pollution. PLoS ONF, 2017, 12, e0172438.	2.5	94

5

#	Article	IF	CITATIONS
73	Predicting total dissolved salts and soluble ion concentrations in agricultural soils using portable visible near-infrared and mid-infrared spectrometers. Biosystems Engineering, 2016, 152, 94-103.	4.3	43
74	Prediction of soil attributes using the Chinese soil spectral library and standardized spectra recorded at field conditions. Soil and Tillage Research, 2016, 155, 492-500.	5.6	71
75	Prediction of soil organic matter using a spatially constrained local partial least squares regression and the <scp>C</scp> hinese vis– <scp>NIR</scp> spectral library. European Journal of Soil Science, 2015, 66, 679-687.	3.9	138
76	Potential of VIS-NIR-SWIR Spectroscopy from the Chinese Soil Spectral Library for Assessment of Nitrogen Fertilization Rates in the Paddy-Rice Region, China. Remote Sensing, 2015, 7, 7029-7043.	4.0	23
77	In Situ Measurements of Organic Carbon in Soil Profiles Using vis-NIR Spectroscopy on the Qinghai–Tibet Plateau. Environmental Science & Technology, 2015, 49, 4980-4987.	10.0	81
78	Effects of sediment texture on in-stream nitrogen uptake. Environmental Earth Sciences, 2014, 72, 21-33.	2.7	1